REMARKS/ARGUMENTS

Reconsideration of this application is requested. Claims 1-5, 8-22, 27-53, 65 and 66 are in the case.

I. ELECTION/RESTRICTION

The election of Group I, claims 1-26, 51-53 and 57, is affirmed. Applicants also affirm the election of the compound of 52 as set forth in paragraph 4 on page 2 of the Action. Non-elected claims 27-50 are withdrawn.

II. THE 35 U.S.C. §112, FIRST PARAGRAPH, REJECTION

Claims 8-21 stand rejected under 35 U.S.C. §112, first paragraph, on lack of enablement grounds for the reasons detailed on page 3 of the Action. In particular, the Action asserts that while the specification is enabling for use of compounds of formula (I) for treating cells *in vitro*, it allegedly does not reasonably provide enablement for use of compounds of the formula (I) for treating cancer (i.e., anti-cancer treatment), *in vivo*. The rejection is respectfully traversed.

The Action asserts, in the paragraph bridging pages 5 and 6, that the only direction or guidance present in the specification is the listing of exemplary *in vitro* invasion assays of cells. This is incorrect. In this regard, attention is directed to Table 4 on pages 61 and 62 of the specification. Table4 gives data showing significant activity of compounds of formula (1) against hypoxic cells in SiHa human cervical carcinoma xenografts in nude mice. Figure 2 also presents data showing *in vivo* activity of the

compound Ib-7P as a nitroreductase activated cytotoxin against human colon carcinoma xenografts in nude mice.

The activity of certain compounds of formula (I) has also been the subject of significant investigation post-filing of the present application. Much of that work has been published, particularly with respect to the elected single species, the compound of claim 52. In this regard, attention is directed to the attached a copy of the following published paper:

> Patterson, A.V., Ferry, D.M., Edmunds, S. j., Gu, Y., Singleton, R. S., Patel, K., Pullen, S., Syddall, S. P., Atwell, 0. J. Yang, S., Denny, W. A., Wilson, W. R. Mechanism of action and preclinical antitumor activity of the novel hypoxia-activated DNA crosslinking agent PR-I 04. *C/in. Cancer Re;, 2007,* 13, 3922-2932.

This paper describes the activity of the compound referred to as PR-104, which is the compound claimed in claim 52 of the present application, in a variety of xenograft models (see Figure 6 and Table 1) *In vivo.* The results in the paper show that PR-104 has marked activity against multiple human tumors in xenograft models in mice.

In light of the above, it is clear that the presently claimed invention is supported by an enabling disclosure, and that one of ordinary skill, as of the filing date of the application could have carried out the invention without the exercise of undue experimentation. Withdrawal of the lack of enablement rejection is accordingly respectfully requested.

III. THE 35 U.S.C. §112, SECOND PARAGRAPH, REJECTION

Claims 23-26 stand rejected under 35 U.S.C. §112, second paragraph, as allegedly indefinite. In response, and without conceding to this rejection, claims 23-26 have been cancelled without prejudice. Withdrawal of the 35 U.S.C. §112, second paragraph, rejection is respectfully requested.

IV. THE 35 U.S.C. §101 REJECTION

Claims 23-26 stand rejected under 35 U.S.C. §101 as not setting forth any process steps. In response, as noted above, claims 23-26 have been cancelled without prejudice. Withdrawal of the 35 U.S.C. §101 rejection is respectfully requested.

V. DOUBLE PATENTING

Claims 1-26, 51-53 and 57 stand provisionally rejected on obviousness-type double patenting grounds as allegedly unpatentable over claim 24 of co-pending application Serial No. 11/654,698 to Patterson *et al.* In response, it is noted that application Serial No. 11/654,698 was filed in the USA on 18 January 2007, claiming priority from a New Zealand application filed on 11 September 2006. The present application has an actual US filing date of 30 April 2006, an effective filing date of 29 October 2004 and claims priority from New Zealand applications filed on 31 October 2003 and 28 September 2004. The present application therefore has earlier priority and filing dates than those of the cited application. Withdrawal of the double patenting rejection is accordingly respectfully requested.

VI. CLAIM OBJECTIONS

Claims 1, 22 and 53 have been objected to because of the use of the term "including". In response, claim 1 has been amended to replace the expression "including" by "selected from". Claims 22 and 53 have been amended to replace the term "including" with "comprising". Similar amendments have been made in other independent claims in the case. No new matter is entered.

Claims 6 and 7 drawn to product by process have been objected to as being substantial duplicates of claims from which they depend. In response, and without conceding to the rejection, claims 6 and 7 have been cancelled without prejudice.

Withdrawal of the claim objections is believed to be in order. Such action is respectfully requested.

Favorable action is awaited.

Respectfully submitted,

NIXON & VANDERHYE P.C.

By: _____
Leonard C. Mitchard
Reg. No. 29,009

LCM:lff
901 North Glebe Road, 11th Floor
Arlington, VA 22203-1808
Telephone: (703) 816-4000
Facsimile: (703) 816-4100

Attachment: Patterson, A.V., Ferry, D.M., Edmunds, S. j., Gu, Y., Singleton, R. S., Patel, K., Pullen, S., Syddall, S. P., Atwell, 0. J. Yang, S., Denny, W. A., Wilson, W. R. Mechanism of action and preclinical antitumor activity of the novel hypoxia-activated DNA crosslinking agent PR-I 04. *C/In. Cancer Re;, 2007,* 13, 3922-2932

Cancer Therapy: Preclinical

Mechanism of Action and Preclinical Antitumor Activity of the Novel Hypoxia-Activated DNA Cross-Linking Agent PR-104

Adam V. Patterson, Dianne M. Ferry, Shelley J. Edmunds, Yongchuan Gu, Rachelle S. Singleton, Kashyap Patel, Susan M. Pullen, Kevin O. Hicks, Sophie P. Syddall, Graham J. Atwell, Shangjin Yang, William A. Denny, and William R. Wilson

Abstract

Purpose: Hypoxia is a characteristic of solid tumors and a potentially important therapeutic target. Here, we characterize the mechanism of action and preclinical antitumor activity of a novel hypoxia-activated prodrug, the 3,5-dinitrobenzamide nitrogen mustard PR-104, which has recently entered clinical trials.

Experimental Design: Cytotoxicity *in vitro* was evaluated using 10 human tumor cell lines. SiHa cells were used to characterize metabolism under hypoxia by liquid chromatography-mass spectrometry, and DNA damage by comet assay and γH2AX formation. Antitumor activity was evaluated in multiple xenograft models (PR-104 ± radiation or chemotherapy) by clonogenic assay 18 h after treatment or by tumor growth delay.

Results: The phosphate ester "pre-prodrug" PR-104 was well tolerated in mice and converted rapidly to the corresponding prodrug PR-104A. The cytotoxicity of PR-104A was increased 10- to 100-fold by hypoxia *in vitro*. Reduction to the major intracellular metabolite, hydroxylamine PR-104H, resulted in DNA cross-linking selectively under hypoxia. Reaction of PR-104H with chloride ion gave lipophilic cytotoxic metabolites potentially able to provide bystander effects. In tumor excision assays, PR-104 provided greater killing of hypoxic (radioresistant) and aerobic cells in xenografts (HT29, SiHa, and H460) than tirapazamine or conventional mustards at equivalent host toxicity. PR-104 showed single-agent activity in six of eight xenograft models and greater than additive antitumor activity in combination with drugs likely to spare hypoxic cells (gemcitabine with Panc-01 pancreatic tumors and docetaxel with 22Rv1 prostate tumors).

Conclusions: PR-104 is a novel hypoxia-activated DNA cross-linking agent with marked activity against human tumor xenografts, both as monotherapy and combined with radiotherapy and chemotherapy.

Hypoxia is a uniquely attractive target in oncology for two reasons. The first is that hypoxic cells are obstacles to curative cancer therapy with all major treatment modalities. Hypoxia can compromise outcomes of surgery by increasing tumor metastasis (1–3). It is also a major cause of radioresistance because oxygen is a radiosensitizer, and multiple clinical studies have documented the importance of hypoxia determining local tumor control in radiotherapy (4–6). Hypoxia also contributes to chemoresistance through multiple mechanisms (7), including limitations on delivery of blood-borne drugs to hypoxic regions of tumors (8, 9). The second reason for targeting hypoxia is that it is a common feature of a wide variety of human tumors and is typically more severe in tumors than in normal tissues, thus providing a basis for tumor selectivity (10, 11).

Several strategies for exploiting tumor hypoxia are now in preclinical or clinical development (7), with the main focus on prodrugs that are activated by metabolic reduction under hypoxic conditions to form cytotoxins. Early efforts focused on quinone bioreductive drugs, such as porfiromycin (12), and 2-nitroimidazole–linked alkylating agents, such as CI-1010 (PD 144872, the *R*-enantiomer of RB 6145; ref. 13), although the latter caused irreversible retinal toxicity in preclinical species (14, 15) and did not proceed to clinical trial. Currently, the hypoxia-activated prodrugs most advanced clinically are *N*-oxides, such as tirapazamine (16) and banoxantrone (17), but are still classified as investigational drugs.

We have identified a further class of hypoxia-activated prodrugs, dinitrobenzamide mustards (DNBM), which seem to offer advantages in preclinical models. DNBM prodrugs contain a latent nitrogen mustard moiety, which becomes activated when either of the nitro groups is reduced to the corresponding hydroxylamine or amine (18). This "electronic switch"

Authors' Affiliation: Auckland Cancer Society Research Centre, School of Medical Sciences, The University of Auckland, Auckland, New Zealand

Received 2/26/07; revised 3/31/07; accepted 4/12/07.

Grant support: Health Research Council of New Zealand (01/276) and Proacta, Inc.

The costs of publication of this article were defrayed in part by the payment of page charges. This article must therefore be hereby marked *advertisement* in accordance with 18 U.S.C. Section 1734 solely to indicate this fact.

Note: Supplementary data for this article are available at Clinical Cancer Research Online (http://clincancerres.aacrjournals.org/).

Requests for reprints: William R. Wilson, Auckland Cancer Society Research Centre, The University of Auckland, Private Bag 92019, Auckland, New Zealand. Phone: 64-9-3737599, ext. 86886; Fax: 64-9-3737671; E-mail: w.wilson@auckland.ac.nz.

doi:10.1158/1078-0432.CCR-07-0478

generates reactive nitrogen mustard metabolites selectively in hypoxic cells, resulting in hypoxia-selective cytotoxicity (19, 20). DNBM prodrugs have two notable features, shown for the prototype of this class, the 2,4-dinitrobenzamide dichloromustard SN 23862. The first is that its activation is confined to lower oxygen concentrations than for tirapazamine (21), which offers the potential for improved selectivity for severe (pathologic) hypoxia in tumors. The second is that its activated metabolites are able to diffuse locally in tumor tissue, providing an efficient bystander effect (killing of untargeted cancer cells; refs. 22, 23). We have shown that, unlike the DNBMs, reductive activation of tirapazamine or the active form of CI-1010 does not provide bystander effects in hypoxic multicellular cultures (21). These features suggest that DNBM prodrugs have unique potential for exploiting tumor hypoxia selectively through the release of activated nitrogen mustards that can also kill adjacent cells at higher oxygen concentrations.

Here, we report the mechanism of action and nonclinical antitumor activity of a new DNBM prodrug, PR-104 (see Fig. 4A for structure), which we have optimized for hypoxic selectivity and *in vivo* antitumor activity. PR-104 combines two key aspects identified by structure-activity relationship studies in the DNBM series; unlike the 2,4-dinitro-5-mustard SN 23862, PR-104 is a 3,5-dinitrobenzamide-2-mustard, which is more readily reduced in hypoxic cells, and its asymmetrical nitrogen mustard contains more reactive leaving groups (bromide and mesylate rather than chloride). We show that PR-104, a water-soluble phosphate "pre-prodrug," is converted efficiently to the more lipophilic DNBM alcohol PR-104A, which is a hypoxia-selective DNA cross-linking agent and cytotoxin. PR-104 shows a higher therapeutic ratio than tirapazamine for killing hypoxic cells in human tumor xenografts but also efficiently kills aerobic cells in tumors as shown by its marked single-agent (monotherapy) activity. PR-104 is currently in a phase I clinical trial, which commenced in January 2006.

Materials and Methods

Compounds. PR-104 [2-((2-bromoethyl)-2-{[(2-hydroxyethyl) amino]carbonyl}-4,6-dinitroanilino)ethyl methanesulfonate phosphate ester] was synthesized, as the free acid, from PR-104A as described (24). The batches used in this study varied in purity from 93% to 98% for PR-104 and 96% to 100% for PR-104A based on high-performance liquid chromatography (HPLC) with absorbance detection (254 nm). The studies on combination with docetaxel and gemcitabine used good manufacturing practices grade PR-104, lot 909-01-001 (purity 97%). Tirapazamine was synthesized in this laboratory (25). Excipient-free chlorambucil, melphalan, cisplatin, and cyclophosphamide were purchased from Sigma-Aldrich, and docetaxel (Aventis Pharma) and gemcitabine HCl (Eli Lilly and Company) as their clinical formulations. Tetradeuterated (d_4) stable isotope standards of PR-104 and PR-104A were synthesized as described (26). The hydroxylamine metabolite of PR-104A, PR-104H, was synthesized by reduction of PR-104A (150 mg) with zinc powder (250 mg) and ammonium acetate (250 mg) in acetone (15 mL). After stirring at room temperature for 4 min, the filtrate was purified by chromatography on silica gel with ethyl acetate/methanol to give PR-104H (123 mg, 85% yield) as a yellow oil. Stock solutions of PR-104H in acetonitrile showed 20% loss over 8 h at room temperature but were stable for >3 months at -80°C.

Cell culture. Cell lines were purchased from the American Type Culture Collection except for gifts of Chinese hamster lines UV4, UV41, and 41cER40.1 from Dr. L.H. Thompson (Lawrence Livermore National Laboratory, Livermore, CA). Cells were passaged in αMEM containing 5% fetal bovine serum without antibiotics for <3 months from frozen stocks confirmed to be *Mycoplasma*-free by PCR-ELISA (Roche Diagnostics).

Inhibition of cell proliferation in vitro. Cells were exposed to compounds (prepared as DMSO stock solutions) in 96-well plates for 4 h under aerobic or hypoxic conditions and grown for 5 days in fresh medium before staining with sulforhodamine B as described previously (25). The IC_{50} was determined by interpolation as the drug concentration reducing staining to 50% of controls on the same plate.

Clonogenic cell killing in single-cell suspensions and spheroids. HCT116 multicellular spheroids were grown in spinner flasks for 10 days (diameter, ~900 μm) and single cells were prepared by dissociating with 0.25% trypsin/EDTA (Life Technologies, Invitrogen). Single cells and intact spheroids were exposed to PR-104A for 4 h as magnetically stirred suspensions (10 mL/bottle), at the same average cell density, in αMEM with 10% fetal bovine serum under flowing 5% CO_2 in air or N_2 in a 37°C waterbath. Drug-treated spheroids were dissociated as above, and cells were washed by centrifugation and plated to determine clonogenic survival.

PR-104A metabolism in stirred cell suspensions. Subconfluent SiHa monolayers in T-175 flasks were harvested (trypsin/EDTA) to prepare suspensions (2-5 × 10^6/mL) in αMEM (8-10 mL), which were exposed to PR-104A as above. Samples were removed at intervals, chilled, and reoxygenated by pipetting rapidly on ice and centrifuged (11,000 × *g* for 30 s in a prechilled rotor). The extracellular medium and extracted cell pellets (50 μL ice-cold methanol per pellet of 2 × 10^6 cells, vortexed for 10 s) were frozen at -80°C for subsequent HPLC. Viability of cells by trypan blue exclusion was in the range 89% to 95% in all samples.

HPLC, mass spectrometry, and bioassay of cellular metabolites. Methanol extracts of SiHa cell pellets were centrifuged (13,000 × *g* for 5 min) and diluted 1:2 with ammonium formate buffer (45 mmol/L, pH 4.5), and samples (100 μL) were analyzed by HPLC with photodiode array and electrospray/single-stage quadrupole mass spectrometer detectors (Agilent 1100/MSD model D, Agilent Technologies) as detailed elsewhere.[1] The isosbestic point for conversion of PR-104A to PR-104H was shown to be 254 nm (data not shown); all metabolites were therefore quantified assuming extinction coefficients equal to PR-104A at this wavelength. Intracellular drug concentrations were calculated using the mean intracellular water volume of SiHa cells determined by Coulter pulse height analysis (mean, 1,776 fL), calibrated against HT29 cells (27). In addition, extracellular medium samples were fractionated by HPLC using an acetonitrile/water gradient and Agilent 1100 fraction collector and bioassayed against UV4 cells (21). Briefly, the eluate was diluted 15-fold into UV4 cultures in 96-well plates and cell densities were determined by sulforhodamine B staining 4 days later.

Single-cell gel electrophoresis (comet assay). SiHa cell suspensions (10^6 cells/mL in αMEM) were exposed to PR-104A under aerobic and hypoxic conditions as above. The effect on DNA breakage induced by cobalt-60 γ-irradiation (10 Gy) was assayed using the alkaline comet assay as previously (28), except that images were analyzed to determine tail moments using Komet v5.0 software (Kinetic Imaging Ltd.).

γH2AX assays. Following drug treatment of stirred cell suspensions as above, cells were grown in as monolayers for 24 h and harvested with trypsin/EDTA. Cytospins were fixed with paraformaldehyde and stained with 4′,6-diamidino-2-phenylindole and then for γH2AX using a phosphorylated-specific mouse monoclonal antibody (Upstate Biotechnology) as described (29) but using an Alexa Fluor 488 goat anti-mouse IgG secondary antibody (Molecular Probes). Slides were viewed with a Leica DMR microscope using a 100× oil immersion objective and a cooled color Nikon digital sight camera. Image

[1] K. Patel et al. Analysis of the hypoxia-activated dinitrobenzamide mustard phosphate prodrug PR-104 and its alcohol metabolite PR-104A in plasma and tissues by liquid chromatography-mass spectrometry, submitted for publication.

fluorescence was quantified using ImageJ software (version 1.37). 4′,6-Diamidino-2-phenylindole–stained nuclei were outlined and overlaid on γH2AX images using Adobe Photoshop (version 5.0 LE). For flow cytometry, cells were fixed in 70% ethanol, rehydrated, and incubated with the above γH2AX antibody (1:500 dilution, 2 h) and secondary (1:400 dilution, 1 h) at room temperature. Cells were resuspended in 1 mL PBS containing 100 μg/mL RNase and 20 μg/mL propidium iodide and analyzed using a Becton Dickinson FACScan with CellQuest software using forward scatter to gate out debris.

Animals, dosing, and toxicology. Specific pathogen-free homozygous nude (CD1-Foxn1^{nu}) mice (Charles River Laboratories) were bred by the Animal Resources Unit (University of Auckland), housed in Techniplast microisolator cages, and fed Harlan Teklad diet 2018l. Animals were identified by ear tags and weighed 18 to 26 g at the time of experiments. All animal studies were approved by the University of Auckland Animal Ethics Committee (approvals R279 and C337). PR-104 free acid was dissolved in PBS + 1 equivalent $NaHCO_3$, or the clinical formulation (PR-104 sodium salt lyophilized with mannitol) was reconstituted in 2 mL water and diluted in PBS. Chlorambucil was dissolved in 0.5 mmol/L $NaHCO_3$ (pH 8.5), tirapazamine in 0.9% NaCl solution + 5% DMSO, melphalan, cyclophosphamide, cisplatin, and gemcitabine in 0.9% NaCl solution, and docetaxel in the manufacturer's diluent. Final concentrations of PR-104, tirapazamine, chlorambucil, and melphalan were determined by spectrophotometry. Dosing solutions were prepared fresh, held at room temperature in amber vials, and used within 3 h. Maximum tolerated dose (MTD) values were determined using 1.33-fold dose escalations. Animals were culled promptly if body weight loss exceeded 15% or there were clinical signs of severe morbidity. The MTD was defined as the highest dose with a frequency of serious toxicity (lethality or cull) <1/6 animals, with a frequency ≥1/6 at the next dose level. To identify dose-limiting toxicities, four male and four female mice were given an ultimately lethal dose of PR-104 (1.78 mmol/kg, i.p.) and culled at 48 h before the onset of significant body weight loss. Histopathology was assessed for 33 tissues/organs (see Supplementary Table S1) using standard formalin-fixed sections with H&E staining. Retinal pathology was evaluated in mice surviving to end point in the MTD studies and quantified by scoring the thickness of the inner and outer nuclear layers as described (15).

Plasma pharmacokinetics. Female mice (three animals per group) were dosed with PR-104 (562 μmol/kg) i.p. or i.v. Blood was collected by cardiac puncture under terminal CO_2 anesthesia into EDTA tubes and chilled, and plasma was prepared by centrifugation (3,000 × *g*, 5 min) and stored at −80°C. The analytic method is described elsewhere.[1] Briefly, thawed plasma was deproteinized with 3 volumes methanol containing d_4-PR-104 and d_4-PR-104A (4 μmol/L each) and 100 μL were analyzed with an Agilent 1100 LC/MSD by monitoring *m/z* values at 579 (PR-104), 585 (d_4-PR-104), 499 (PR-104A), and 505 (d_4-PR-104A). Noncompartmental pharmacokinetic variables were estimated using WinNonlin version 4.0.1; area under the curve values were calculated using the log trapezoidal rule with extrapolation of the terminal slope to infinity by linear regression.

Tumor excision assays. Tumors were grown s.c. in the flank by inoculating cells grown in tissue culture (10^7 cells in 100 μL αMEM). Tumors were monitored using electronic calipers. When tumors reached treatment size (mean, 517; SD, 249 mm^3), mice were randomized to treatment groups (five to seven per group). Compounds were given as single i.p. doses alone or 5 min after whole body irradiation (^{60}Co source). Eighteen hours after treatment, tumors were excised, weighed, minced, dissociated enzymatically, and plated to determine clonogenicity as described (9). Clonogens/gram of tissue were calculated relative to controls and effects of treatment were tested for significance (ANOVA with Dunnett's).

Tumor growth delay assays. All experiments were done in CD-1 nude mice, except Panc-01 growth delay, which was done in ICR severe combined immunodeficient mice by TGen Drug Development Services. Animals were randomized to treatment groups (five to nine mice per group) when tumors reached treatment size (mean, 233; SD, 87 mm^3). Tumor size and body weight were determined thrice weekly. Tumor volume was calculated as $\pi (L \times w^2) / 6$, where L is the major axis and w is the perpendicular minor axis. Animals were culled 100 days after start of treatment or when mean tumor diameter exceeded 15 mm. Treatment efficacy was assessed by comparing survival with controls using the log-rank test or by post hoc ANOVA (Holm-Sidak test) when multiple groups were compared (SigmaStat v3.10). In addition, the median time for tumors to increase in volume 4-fold relative to pretreatment volume (RTV-4) was determined, and the specific growth delay (SGD) was calculated as the percentage increase in RTV-4 for treated versus control. This variable normalizes for differences in tumor volume at treatment and for differences in control tumor growth rate between cell lines. Long-term controls (time to end point, >100 days) were assigned an RTV-4 value of 100 days, and significance of drug effects was tested using the Mann-Whitney *U* test (SigmaStat v3.10).

Results

Hypoxia-selective cytotoxicity of PR-104A. The antiproliferative potency of PR-104A was compared with chlorambucil and tirapazamine by determining IC_{50} values in a panel of 10 human carcinoma cell lines following 4-h drug exposures under aerobic and hypoxic conditions (Fig. 1A and B). Under hypoxia (<10 ppm O_2 gas phase), PR-104 varied in potency between cell lines, with the lowest IC_{50} (0.51 μmol/L) in H460 non–small cell lung cancer cells and highest (7.3 μmol/L) in PC3 prostate cells. Its potency was slightly greater than tirapazamine in most cell lines and up to 10-fold greater than chlorambucil (Fig. 1A). The hypoxic selectivity of PR-104A, measured as the ratio of IC_{50} values under aerobic and hypoxic conditions (Fig. 1B), was ~100-fold for HCT116, C33A, and H1299 cells and ~10-fold for the other cell lines. Tirapazamine showed consistently high hypoxic selectivity (~100-fold) in all cell lines, whereas chlorambucil lacked hypoxic selectivity. The hypoxic selectivity of PR-104A was confirmed by clonogenic assay against stirred suspensions of HCT116 cells, which indicated a similar hypoxic cytotoxicity ratio (30-fold) whether cells were exposed in multicellular spheroids or as single cells from enzymatically dissociated spheroids under equivalent ambient conditions (Fig. 1C).

Reductive metabolism of PR-104A. We evaluated metabolism of PR-104A in aerobic and hypoxic suspensions of SiHa cells by liquid chromatography-mass spectrometry; a summary of the identified metabolites is provided in Fig. 2A, a representative chromatogram in Fig. 2B, and the time course for intracellular metabolites (extracted with methanol) and extracellular metabolites (by direct analysis of medium) in Fig. 2C. PR-104A was lost from the extracellular medium at a faster rate in hypoxic cultures (first-order rate constant, 0.23 ± 0.01 h^{-1} versus 0.045 ± 0.005 h^{-1} under aerobic conditions; data not shown). The major intracellular metabolite under hypoxia was the hydroxylamine PR-104H (base peak *m/z* 485 by positive mode electrospray ionization, corresponding to the M+H$^+$ ion, with an isotope pattern showing 1 Br; representative mass spectra are provided in Supplementary Fig. S1 and variables are summarized in Supplementary Table S2). Zinc dust reduction of PR-104A gave a species identical to the PR-104H metabolite (by retention time, absorbance, and mass spectrum). The ^{1}H-^{15}N gradient-enriched heteronuclear multiple bond correlation nuclear magnetic resonance spectrum of synthetic PR-104H (see Supplementary Fig. S2), showing coupling

between the nitro group N and proton of the CH *para* to the carboxamide and couplings of the hydroxylamine N with both CH protons. This unambiguously identified the position of the hydroxylamine as *para* to the nitrogen mustard. PR-104H reached its maximum concentration at 1 h and was present at 10- to 20-fold lower concentrations in aerobic cells (Fig. 2C).

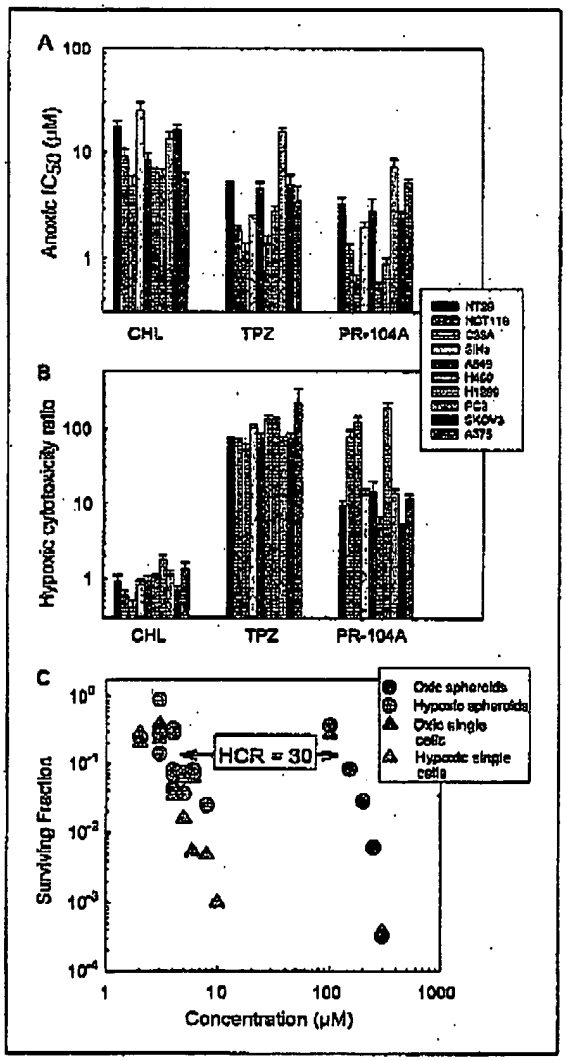

Fig. 1. Hypoxia-selective cytotoxicity of PR-104A against human tumor cell lines *in vitro*. *A*, IC_{50} values for 4-h exposure under hypoxia conditions. Columns, mean for multiple (median, 5) experiments with each cell line; bars, SE. CHL, chlorambucil; TPZ, tirapazamine. *B*, hypoxic cytotoxicity ratios (aerobic IC_{50}/hypoxic IC_{50}) from the same experiments. *C*, clonogenic survival curves for HCT116 colon carcinoma cells exposed to PR-104A for 4 h as single cells or multicellular spheroids in stirred suspensions under the same ambient conditions. Values are pooled from three experiments.

A complex set of minor products (compounds 1-4) in SiHa cells, detected only under hypoxia, was formed with slightly slower kinetics. These had absorption spectra very similar to PR-104H and mass spectra consistent with displacement of either the bromo or mesylate leaving group of PR-104H by chloride or hydroxide ion, giving 1 (*m/z* 425; 1 Cl + 1 Br isotope pattern), 2 (*m/z* 441; 1 Cl), 3 (*m/z* 381; 2 Cl), and 4 (*m/z* 407; 1 Br). A common hydrolysis product of 1 to 3, compound 5 (*m/z* 363; 1 Cl), was detected but not resolved chromatographically from 9. In addition, a metabolite in hypoxic cells formed with similar kinetics to PR-104H and had a mass spectrum (*m/z* 469; 1 Br) consistent with the corresponding amine (6). Its identity was confirmed by its presence as a minor product in the zinc dust reduction of PR-104A and its slow autoxidation to PR-104H. Its nucleophilic displacement products 7 (*m/z* 365; 2 Cl), not chromatographically resolved from 1, and 8 (*m/z* 347; 1 Cl) were also detected.

In addition, two metabolites that we interpret as arising from reduction of the nitro group *ortho* to the mustard moiety were detected only under hypoxia. Compound 9 had a mass spectrum (*m/z* 373; 1 Br) consistent with cyclization via intramolecular alkylation of the *ortho* hydroxylamine by the mesylate leaving group of the mustard to form a tetrahydroquinoxaline (as reported following *ortho* nitroreduction of the dinitrobenzamide chloromustard SN 23862 (21, 30)]. The corresponding hydrolysis product 10 (*m/z* 311, no halogens) showed an absorbance spectrum distinct from the *para* nitroreduction products (Supplementary Fig. S1) and increased linearly with time consistent with its formation as a stable end product.

Certain of the reduced metabolites were also detected in extracellular medium (Fig. 2C, *right*). The extracellular metabolite profile was biased, relative to that within cells, in favor of the more lipophilic metabolites. Thus, the mesylate-containing PR-104H was present at ~100-fold lower concentrations than in the cells, and the corresponding amine 6 was not detected, whereas the more lipophilic chlorodisplacement products 1 and 3 and the tetrahydroquinoxaline 10 were relatively prominent. This is consistent with more efficient passive diffusion of lipophilic reduction products out of the cells.

We investigated the bioactivity of reduction products in extracellular medium, after incubation of hypoxic SiHa cells with PR-104A for 3 h, by assaying the HPLC fractions for inhibition of proliferation of the *ERCC1* mutant UV4 (Fig. 2B, *bottom*). This showed two new peaks of bioactivity, in addition to PR-104A. The earlier eluting peak corresponded to the dichlorohydroxylamine 3 and the later peak to the bromohydroxylamine/chlorohydroxylamine 1 and/or the dichloroamine 7 (which were not resolved).

PR-104A is a hypoxia-selective DNA-damaging agent. DNA cross-linking in SiHa cells following exposure to PR-104A was shown by single-cell gel electrophoresis (comet assay), which showed little or no effect of drug only (data not shown) but greater suppression of radiation-induced DNA single-strand breaks (i.e., greater interstrand cross-linking) under hypoxic than aerobic conditions (Fig. 3A). We also showed that UV41 cells, which are defective in DNA interstrand cross-link repair by virtue of mutation of XPF/ERCC4 (31), are hypersensitive to the major hypoxic metabolite of PR-104A, the *para* hydroxylamine PR-104H (Fig. 3B). The hypersensitivity of UV41 relative

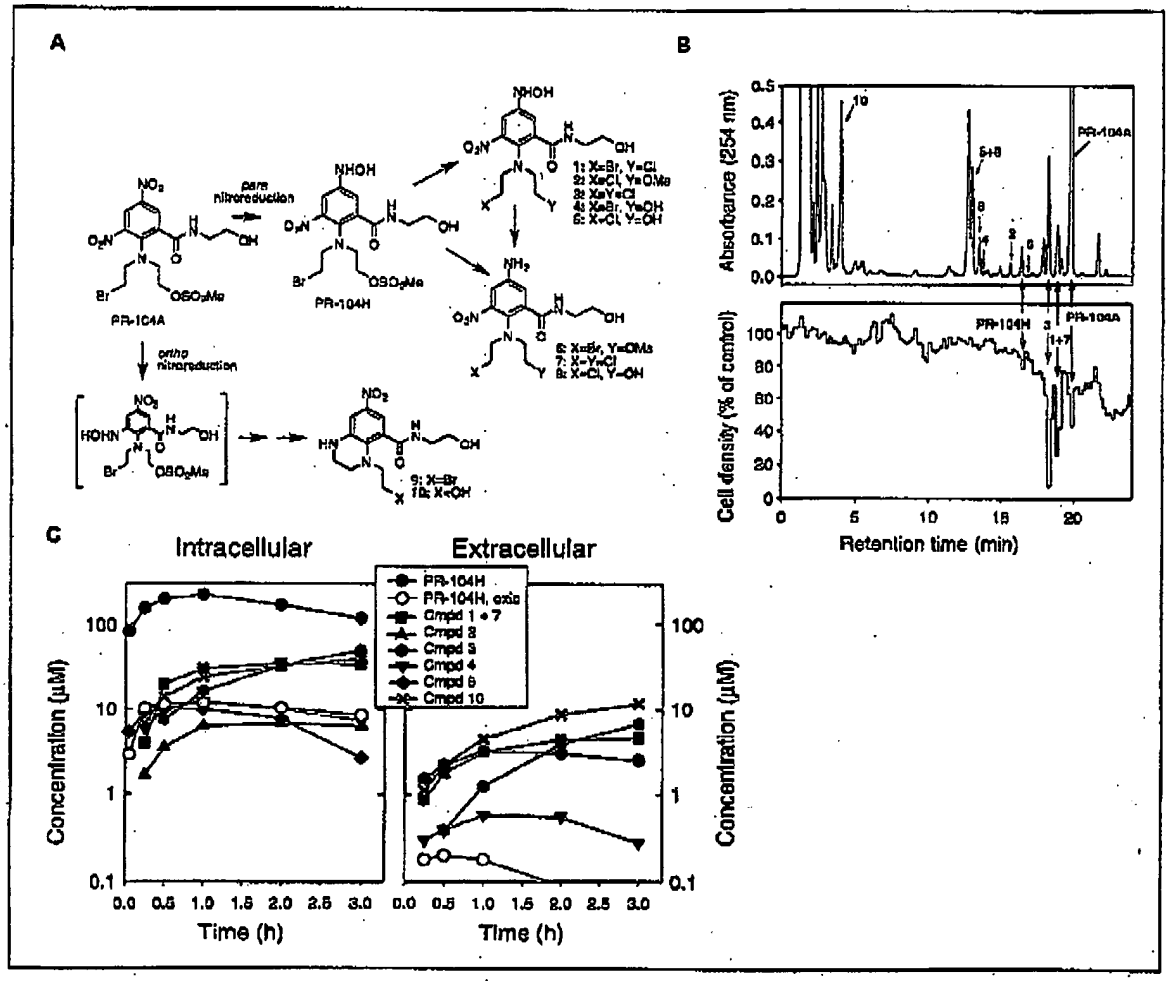

Fig. 2. Metabolites in stirred SiHa cell suspensions incubated with PR-104A under hypoxia. *A*, metabolites identified by on-line mass spectrometry and (for PR-104A and PR-104H) by comparison of retention time and absorbance spectra with authentic standards. *B*, HPLC of extracellular medium after incubation at 5×10^6 cells/mL with 300 μmol/L PR-104A for 3 h. The upper trace shows absorbance and lower trace shows bioactivity of HPLC fractions against UV4 cells. *C*, time course of intracellular and extracellular metabolites for 200 μmol/L PR-104A at 2×10^6 cells/mL. Quantitation by absorbance. Points, mean of two experiments. Ranges (omitted for clarity) averaged 12% of the mean across all analytes.

to 41cER40.1, a human XPF transfectant restoring 90% of XPF activity to UV41 (32), was 21-fold under aerobic conditions and 28-fold under hypoxia. The UV41/41cER40.1 differentials for PR-104H were similar to those for chlorambucil (Fig. 3B), consistent with cytotoxicity of PR-104H being due predominantly to DNA cross-linking.

Incubation of SiHa cells following exposure to PR-104A resulted in phosphorylation of Ser^{139} of histone H2AX (γH2AX), which was more prominent following hypoxic than aerobic exposure (Fig. 3C). Image analysis showed a 2.5-fold increase in the geometric mean integrated fluorescence per nucleus after hypoxic versus aerobic exposure. A similar differential was shown by flow cytometry (Fig. 3D). Chlorambucil also caused H2AX phosphorylation but in an oxygen-independent manner (Fig. 3D). The γH2AX response to both drugs occurred with delayed kinetics, reaching a maximum at ~24 h and was accompanied by accumulation of cells with an S-phase DNA content (data not shown). Thus, γH2AX induction may be due, in part, to arrest of replication forks at DNA interstrand cross-links.

PR-104 is well tolerated in mice and rapidly converted to PR-104A. PR-104A had limited aqueous solubility (1.66 mmol/L in culture medium); a water-soluble phosphate ester, PR-104, was therefore prepared as a pre-prodrug to release PR-104 via systemic phosphatases (Fig. 4A). Titration of the PR-104–free acid with one equivalent of sodium bicarbonate gave an

aqueous solubility of >200 mmol/L. The MTD of PR-104 as a single i.p. dose in nude mice was 1.33 mmol/kg i.p., equivalent to 770 mg/kg of the free acid (molecular weight, 579.28). MTD values for the other agents investigated (in mmol/kg) were 0.750 for cyclophosphamide, 0.237 for chlorambucil, 0.0422 for melphalan, 0.178 for tirapazamine, 0.0316 for cisplatin, 0.10 for docetaxel, and 1.0 for gemcitabine.

Facile conversion of the phosphate, PR-104, to its alcohol PR-104A (identified by retention time, absorbance spectrum, and mass spectrum) in mice was shown by liquid chromatography-mass spectrometry of plasma (Fig. 4B). Following i.v. dosing, PR-104 was cleared with an initial half-life of ~3 min; PR-104A was the major species after 5 min and had a terminal half-life of 15 min. Clearance of PR-104 was slower after i.p. dosing, suggesting rate-limiting absorption from the peritoneum, but the plasma area under the curve of PR-104A after i. p. PR-104 (62 μmol-h/L) was 78% of that after i.v. PR-104 (area under the curve, 80 μmol-h/L). I.p. dosing was therefore used for therapeutic studies in mice.

Histopathology 48 h after an ultimately lethal dose of PR-104 identified mucosal cell degeneration/regeneration in the small intestines, particularly the ileum, as the dominant finding in seven of eight mice. This was usually associated with mild to moderate mucosal cell hypertrophy, although no overall loss of mucosal epithelium was found. In addition, a moderate decrease in bone marrow cellularity was seen in all animals, particularly the erythroid series and megakaryocytes. There were no other pathology findings, and in animals surviving to the end of MTD experiments (28 days), no loss of photoreceptor cells in the retina was evident, which contrasts our findings with tirapazamine and CI-1010 (15).

Aerobic and hypoxic cell killing by PR-104 in human tumor xenografts. We first assessed the antitumor activity of PR-104 by excision assay, determining clonogenic cell survival 18 h after giving the drug alone or following a single dose of ionizing radiation (15-20 Gy) to sterilize aerobic tumor cells (Fig. 5A). Using doses at 75% (SiHa and H460) or 100% (HT29) of MTD, PR-104 was active as monotherapy against SiHa, HT29, and H460 xenografts (each $P < 0.01$), but neither chlorambucil nor tirapazamine provided significant single-agent activity. PR-104 showed even greater activity when combined with radiation, with cell killing at or beyond the dynamic range of the assay for all three tumor types. Tirapazamine showed modest but statistically significant ($P < 0.01$) activity after radiation in all three tumors, whereas chlorambucil failed to reach significance for SiHa and H460. These results indicate that PR-104 has marked activity against both radiobiologically hypoxic and aerobic cells in SiHa, HT29, and H460 tumor xenografts at well-tolerated single doses. Further studies with the SiHa tumor, a well-characterized model with respect to hypoxic cell content (33, 34), using PR-104 at 0.266 mmol/kg (20% of its MTD), confirmed its activity after irradiation ($P < 0.001$) and showed that the three reference nitrogen mustards lacked activity against hypoxic cells at 20% of their respective MTD values (Fig. 5B).

Antitumor activity of PR-104 monotherapy in tumor growth delay assays. The notable activity of PR-104 as a single agent by tumor excision assay led us to evaluate its activity using a tumor growth delay end point. To test whether PR-104 monotherapy is schedule dependent, we compared a daily (qd × 14) versus weekly (qw × 3) schedule against the chemoresistant H460 xenograft model using the same total

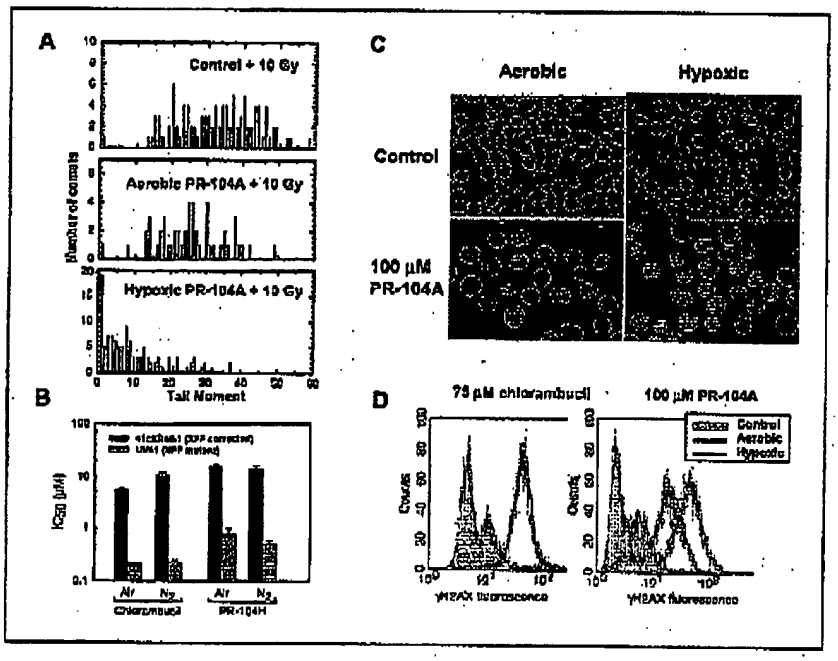

Fig. 3. Hypoxia-selective DNA damage by PR-104A. *A*, alkaline comet assay for DNA single-strand breaks in SiHa cells exposed to PR-104A (30 μmol/L) for 1 h under aerobic or hypoxic conditions. DNA interstrand cross-linking is enhanced under hypoxia as shown by greater suppression of radiation-induced DNA breaks. *B*, antiproliferative activity (IC_{50} values) of chlorambucil and PR-104H after 4-h drug exposure of UV41 and its XPF-restored counterpart (41cER40.1) under aerobic and hypoxic conditions. *C*, SiHa cells immunostained for γH2AX 24 h after a 1-h aerobic or hypoxic exposure to 100 μmol/L PR-104A. Nuclear outlines (*white*) were defined by 4′,6-diamidino-2-phenylindole counting. *D*, flow cytometry profiles of γH2AX in SiHa cells 24 h after 1-h aerobic or hypoxic exposure to chlorambucil (75 μmol/L) or PR-104A (100 μmol/L).

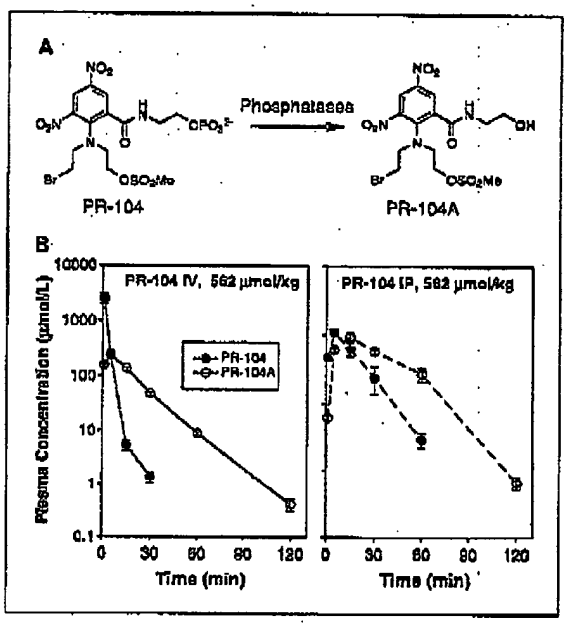

Fig. 4. Pharmacokinetics of PR-104 in CD-1 *nu/nu* mice. *A*, structure of the phosphate pre-prodrug PR-104 and its major plasma metabolite PR-104A. *B*, plasma pharmacokinetics following i.v. or i.p. dosing with PR-104 at 0.55 mmol/kg, determined by liquid chromatography–mass spectrometry using tetradeuterated internal standards. Points, mean for three animals per point; bars, SE.

dose (3.2 mmol/kg) over 14 days, which was well tolerated using both schedules (Fig. 6A). Both schedules were highly active ($P < 0.001$, log-rank test), extending median survival by 22.5 and 33.5 days, respectively, each providing two of nine long-term controls and SGD of 450% and 300%, respectively ($P < 0.001$ with respect to controls). The difference in survival probability in the two schedules was not significant. We further compared PR-104 versus four widely used chemotherapy drugs (docetaxel, cisplatin, gemcitabine, and cyclophosphamide) against H460 tumors with a q4d × 3 schedule (Fig. 6B) using each agent at its MTD (or 56% of MTD in the case of gemcitabine). H460 xenografts showed significant sensitivity only to PR-104; this schedule gave comparable activity to the qw × 3 and qd × 14 schedules used in Fig. 6A.

Given this strong antitumor activity against H460, we tested seven additional xenograft models using the q4d × 3 schedule with a total dose of 3.2 mmol/kg, which was the MTD for this schedule. As summarized in Table 1, six of the eight models showed statistically significant improvement in survival, as determined by log-rank test, with increases in median survival ranging from 8 to >77 days. Overall, there were 7 of 65 (10.8%) long-term controls. These observations were corroborated by statistically significant SGDs in six of the eight models (see Supplementary Fig. S3 for examples of growth delay curves, which are shown for H460, HT29, and A2780 tumors).

Antitumor activity of PR-104 in combination with gemcitabine or docetaxel. The poor tissue penetration of some chemotherapy agents (8) has the potential to spare hypoxic tumor cells. We therefore hypothesized that addition of PR-104 to drugs with suboptimal extravascular transport properties would improve treatment outcome. Gemcitabine has been reported to be least effective against cells in or adjacent to hypoxic regions of tumors (35). We therefore tested the combination of gemcitabine and PR-104 against the human pancreatic xenograft model Panc-01 (Fig. 6C). Gemcitabine was active as a single agent, increasing median survival by 11 days ($P < 0.001$, log-rank test; SGD of 61%; $P = 0.001$). PR-104 possessed comparable single-agent activity in this line (median survival, 11 days; $P < 0.001$, log-rank test; SGD, 30%; $P = 0.024$). The combination provided therapeutic activity greater than either agent alone, with a median survival of 32 days ($P < 0.001$, log-rank test) with tumor regression in eight of nine animals (SGD, 152%; $P < 0.001$; tumor growth curves are shown in Supplementary Fig. S4A). Post hoc ANOVA (Holm-Sidak method) confirmed the survival probability for the combination group as significantly different from either single agent ($P < 0.01$).

Finally, we evaluated docetaxel using the androgen-refractory human prostate xenograft 22RV1. The high molecular weight and target avidity of taxanes is likely to limit their tissue penetration (36, 37). Moderate antitumor activity was seen for either docetaxel or PR-104 alone, with median survival increases of 14.5 and 17 days ($P < 0.001$), respectively, and corresponding SGDs of 122% ($P = 0.014$) and 156% ($P = 0.001$). Coadministration of docetaxel and PR-104 provided a 68-day improvement in median survival ($P < 0.001$) with tumor regression in nine of nine animals (tumor growth curves are shown in Supplementary Fig. S4B), three of which (33%) failed to regrow by day 100 (SGD, 689%; $P < 0.001$). Post hoc ANOVA confirmed the significance of the combined agent therapeutic gain ($P < 0.01$).

Discussion

This study describes a nitrogen mustard pre-prodrug, PR-104, designed to target tumor hypoxia through its selective metabolism to an activated DNA cross-linking agent. We show that PR-104 is a two-stage prodrug system; PR-104 itself is a water-soluble phosphate ester, readily formulated at high concentrations, which is rapidly hydrolyzed *in vivo* to the less soluble alcohol metabolite PR-104A (Fig. 4). The latter is sufficiently lipophilic to penetrate through multiple layers of tumor cells, required to reach hypoxic target cells, as shown by its equivalent cytotoxicity against intact and dissociated multicellular spheroids (Fig. 1C). The alcohol PR-104A is a hypoxia-activated prodrug, shown by its selective metabolic reduction (Fig. 2), DNA damage (Fig. 3), and cytotoxicity (Fig. 1) under hypoxic conditions.

The key metabolite from PR-104A in hypoxic cells, PR-104H, was identified as the hydroxylamine resulting from reduction of the nitro group *para* to the mustard moiety. Steady-state concentrations of PR-104H in hypoxic SiHa cells were 10- to 20-fold higher under hypoxic than aerobic conditions (Fig. 2C), similar to the hypoxic cytotoxicity differential in this cell line (Fig. 1B). This is consistent with cytotoxicity occurring predominantly through this pathway under both aerobic and hypoxic conditions. Tetrahydroquinoxaline metabolites from *ortho* nitroreduction and intramolecular alkylation [as reported previously for the prototype DNBM SN 23862 (21, 30)] were

also detected in SiHa cells (compounds 9 and 10 in Fig. 2A). The *ortho* nitroreduction pathway generates a monofunctional mustard and is unlikely to contribute to cytotoxicity (30), but its stable end product 10 may be a useful biomarker for hypoxic activation of PR-104A.

We also detected multiple products arising from PR-104H (and the minor amine metabolite 6) by replacement of the mustard leaving groups with Cl^- or OH^- (compounds 1-5, 7, and 8). The absence of analogous products from PR-104A itself, despite its much higher concentration, is clear evidence that reduction of the nitro group activates the nitrogen mustard moiety to nucleophilic displacement. This confirms the original design concept for hypoxic activation of nitroaromatic mustards, which was to exploit the large change in electron density on the mustard nitrogen afforded by the biotransformation of an electron-withdrawing nitro group to an electron-donating hydroxylamine or amine (38). This electronic switch presumably contributes to the greater cytotoxicity of the reduced extracellular metabolites 1, 3, and 7 than PR-104A, relative to their molar concentrations, in the bioassay study (Fig. 2B).

The preliminary investigation of DNA damage by PR-104A reported here suggests that DNA interstrand cross-linking is the major mechanism of cytotoxicity. PR-104A forms cross-links in SiHa cells selectively under hypoxia (Fig. 3A), and its major hypoxic metabolite PR-104H shows hypoxia-independent selective toxicity to UV41 cells defective in DNA interstrand cross-link repair (Fig. 3B). The quantitative relationship between cytotoxicity and cross-link formation has yet to be established, but the latter is a potential response biomarker with utility during clinical development of nitrogen mustard prodrugs (39). Of note, Ser^{139} phosphorylation of histone H2AX to form γH2AX, a well-established biomarker of double-strand break formation (40), was shown with both PR-104A and chlorambucil, with a greater response to PR-104 but not chlorambucil under hypoxia. To our knowledge, γH2AX induction by nitrogen mustards has not previously been reported in tumor cells. Further studies are needed to determine whether this reflects collapse of replication forks at cross-links and whether γH2AX has potential as a pharmacodynamic biomarker. A possible limitation in this context is that the enhancement in γH2AX response to PR-104A by hypoxia (Fig. 3C and D) seemed to be less than that for cytotoxicity (Fig. 1C), which may reflect complicating effects on cell cycle progression and replication fork arrest.

It is noteworthy that PR-104H itself makes little contribution to bioactivity in the extracellular medium, relative to the more lipophilic metabolites in which Cl (hydrophobicity substituent constant $\pi = 0.71$) replaces the mesylate group ($\pi = -0.88$). This is consistent with the relatively low cytotoxic potency of exogenously added PR-104H (slightly less than chlorambucil) when added to UV41 cultures (Fig. 3B). We infer that the cytotoxicity of the extracellular metabolites of PR-104 reflects their membrane transport properties as well as their reactivities. The picture that emerges is of a small family of oxygen-insensitive activated metabolites of PR-104A in hypoxic cells, with a range of tissue diffusion properties, and that the more lipophilic metabolites, such as 1, 3, and 7, are likely to be the dominant mediators of bystander effects in tumors.

Frankly toxic doses of PR-104 (1.78 mmol/kg; i.p.) in athymic CD-1 mice identified gastrointestinal toxicity and bone marrow hypocellularity as probable dose-limiting toxicities. No retinal changes were evident, indicating this physiologically hypoxic normal tissue is insensitive to PR-104A [unlike tirapazamine and CI-1010 (15)], consistent with recent studies showing that the O_2 concentration for 50% inhibition PR-104A cytotoxicity in SiHa cultures is 10-fold

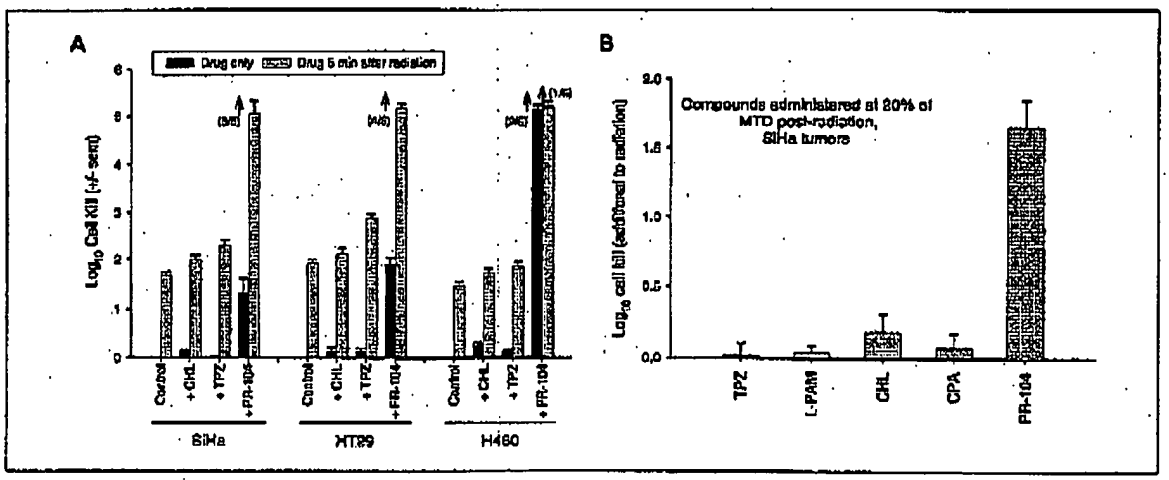

Fig. 6. Antitumor activity of PR-104 against s.c. human tumor xenografts by *ex vivo* clonogenic assay 18 h after single i.p. doses. *A*, PR-104 compared with chlorambucil and tirapazamine, each at 75% (SiHa and H460 tumors) or 100% of MTD (HT29 tumors) given alone or 5 min after γ-irradiation (15 Gy for SiHa and H460 and 20 Gy for HT29). Columns, geometric mean for five to six tumors/group; bars, SE. Means were calculated by assuming one clonogen/3 × 10^5 cells (total number of cells plated) for tumors from which no clonogens were detected; the proportion of tumors below this limit of detection is shown in brackets. *B*, activity against SiHa tumors of tirapazamine, melphalan (*L-PAM*), chlorambucil, cyclophosphamide (*CPA*), or PR-104 at 20% of their respective MTD values 5 min after irradiation (15 Gy).

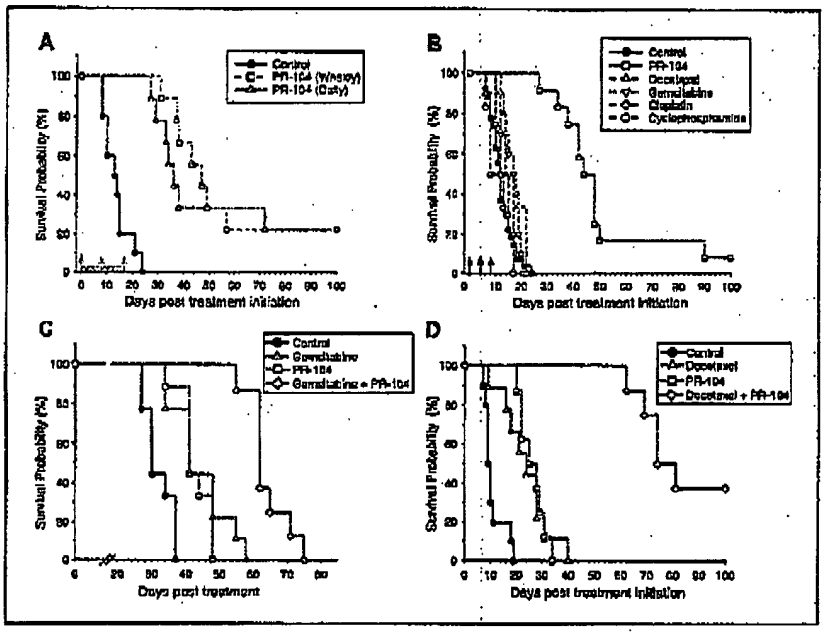

Fig. 6. Kaplan-Meier survival plots depicting single-agent activity of PR-104 (*A* and *B*) and combination chemotherapy activity (*C* and *D*) by i.p. dosing against s.c. xenografts in CD1-Foxn1^{nu} mice. *A*, monotherapy activity of PR-104 with daily (0.23 mmol/kg/dose; qd × 14) or weekly (1.07 mmol/kg/dose; qw × 3) dosing schedules against H460 xenografts. *B*, comparison of PR-104 (1.07 mmol/kg/dose) with docetaxel (0.024 mmol/kg/dose), gemcitabine (0.42 mmol/kg/dose), cisplatin (0.0075 mmol/kg/dose), and cyclophosphamide (0.80 mmol/kg/dose) against H460 xenografts using a q4d × 3 schedule. All compounds were given at their respective MTD for this schedule, except gemcitabine (56% of MTD). *C*, antitumor efficacy of gemcitabine (0.34 mmol/kg/dose), PR-104 (0.52 mmol/kg/dose), or the coadministered combination against Panc-01 pancreatic xenografts using a q4d × 3 schedule. *D*, antitumor efficacy of docetaxel (0.042 mmol/kg/dose), PR-104 (0.56 mmol/kg/dose), or the coadministered combination against 22RV1 androgen-refractory prostate xenografts using a q2w × 3 schedule.

lower than for tirapazamine.[3] This requirement for severe hypoxia for PR-104A activation may contribute to its excellent *in vivo* tolerance at high dose.

I.p. administration of the phosphate pre-prodrug PR-104 to mice, at 42% of its MTD, provided area under the curve values for PR-104A in plasma of mice (62 μmol-h/L) well in excess of that required for hypoxic cytotoxicity in a human tumor cell line panel *in vitro* (Fig. 1A; area under the curve values at IC_{50} from 2.1 to 50 μmol-h/L). Consistent with this, PR-104 showed marked activity against hypoxic cells in multiple human tumor xenograft models (Fig. 5). A striking aspect of the data is that PR-104 was much more active than tirapazamine against hypoxic cells (i.e., when given after a large dose of radiation to sterilize aerobic cells) in the three tumor models in which these agents were compared (SiHa, HT29, and H460; Fig. 5), yet PR-104A was no more potent and was less hypoxia selective than tirapazamine against these same cell lines *in vitro* (Fig. 1A and B). This disparity may reflect, in part, the limited ability of tirapazamine to penetrate into hypoxic regions of tumors (9), along with the 7.5-fold higher molar dose of PR-104 achievable in mice. PR-104 was also much more active than conventional nitrogen mustards (melphalan, chlorambucil, and cyclophosphamide) at equivalent fractions of their respective MTDs in killing hypoxic cells in SiHa tumors (Fig. 5B).

Further, PR-104 (but not tirapazamine) showed substantial activity as monotherapy using either excision assays (Fig. 5) or tumor growth delay end points (Table 1; Fig. 6). This shows that PR-104 kills the aerobic subpopulation as well as hypoxic cells in these tumors. It is not yet clear to what extent this reflects the operation of a bystander effect (hypoxic metabolites diffusing into adjoining aerobic regions) or whether the very high systemic exposures to PR-104A that can be achieved are sufficient to kill aerobic cells directly. The importance of direct activity against aerobic cells is suggested by an apparent correlation between aerobic sensitivity *in vitro* (Fig. 1) and monotherapy antitumor activity (Table 1); the three lines showing the largest tumor responses (H460, SiHa, and HT29) had high hypoxic IC_{50} values and low aerobic IC_{50} values relative to the two cell lines that were less responsive *in vivo* (H1299 and C33A). Single-agent activity has also been noted for VPN40541 (41), an analogue of KS119W that is a nitroaromatic prodrug of a sulfonylhydrazine DNA cross-linking agent (42). The ability of nitrogen mustards, and other cross-linking agents with long-lived DNA lesions, to cause cell cycle–independent cytotoxicity may underlie their utility in killing slowly cycling hypoxic cells in tumors. This is also consistent with the apparent schedule independence of PR-104A as monotherapy, which showed similar activity when the same total dose was given on a daily or weekly schedule. The single-agent activity of PR-104 against H460 tumors refractory to docetaxel, cisplatin, gemcitabine, and cyclophosphamide (Figs. 5A and 6A and B) is particularly striking and suggests that intratumor activation of nitrogen mustards using hypoxia targeting can overcome the treatment-refractory nature of this tumor (43, 44).

Despite this notable monotherapy activity, the therapeutic advantage of hypoxia-activated prodrugs is expected to be greatest in combination with agents that spare hypoxic cells as reported in preclinical models for tirapazamine (45), CI-1010 (13), banoxantrone (AQ4N; ref. 17), and NLCQ-1 (46) with

[3] Hicks KO, Myint H, Patterson AV, et al. Oxygen dependence and extravascular transport of hypoxia-activated prodrugs: comparison of the dinitrobenzamide mustard PR-104A and tirapazamine. Int J Radiat Oncol Biol Phys, in press, 2007.

Table 1. Monotherapy (single agent) activity of i.p. PR-104 using a q4d × 3 schedule (1.07 mmol/kg/dose) against human tumor xenografts in CD-1 nude mice

Tumors and size at treatment			Survival			Tumor growth inhibition	
Xenograft	Tissue origin	Tumor volume, mean ± SD (mm^3)	Median life extension (days)	Long-term controls*	Log rank (P)	SGD (%)†	Mann-Whitney test (P)
H460‡	Lung	218 ± 126	35	1/12	<0.001	400	<0.001
H1299	Lung	310 ± 61	8	2/6	0.012	40	0.527
HT29	Colon	296 ± 51	39	0/6	0.002	192	0.004
SiHa	Cervix	254 ± 33	>77	3/6	0.012	531	0.009
C33A	Cervix	252 ± 45	5	0/7	0.056	53	0.006
MiaPaCa-2	Pancreas	329 ± 65	12	0/5	0.514	61	0.151
Panc-01	Pancreas	165 ± 46	21	0/8	<0.001	94	<0.001
A2780‡	Ovary	254 ± 80	26	1/15	<0.001	460	<0.001

*Tumors nonpalpable or below end point size (mean diameter, 15 mm) at 100 d.
†SGD (median tumor growth delay as a % of median time for controls to reach end point; see Materials and Methods).
‡Pooled analysis of two experiments.

radiation or cytotoxic chemotherapy. The supra-additive activity of PR-104 when combined with gemcitabine and with docetaxel in two different tumor models (Fig. 5B and C) points to this potential. The use of gemcitabine and docetaxel in the treatment of severely hypoxic tumors, such as carcinoma of the pancreas (47, 48) and prostate (5, 49, 50), suggests that clinical benefit could be derived from the addition of a hypoxia-activated prodrug, such as PR-104, to standard of care.

Overall, the nonclinical studies reported here show that PR-104 has marked activity against multiple human tumor xenograft models. This therapeutic activity is seen when PR-104 is used as monotherapy or in combination with agents for which hypoxic cells are likely to limit therapeutic response (illustrated by radiotherapy and docetaxel or gemcitabine chemotherapy). Our working model is that the efficacy of PR-104 reflects two key features we have sought to design into the DNBM class of hypoxia-activated prodrugs. The first is an efficient bystander effect, the possibility of which is suggested by identification of cytotoxic, oxygen-stable lipophilic extracellular metabolites of PR-104A in hypoxic tumor cell cultures (Fig. 2). Analogous metabolites of earlier DNBM prodrugs have been shown to give efficient bystander effects when reduced by *Escherichia coli* NTR (22, 23) or by endogenous reductases in tumor cells (21). The second feature is the restriction of metabolic activation to severe (pathologic) hypoxia to minimize activation in physiologically hypoxic normal tissues. We have recently shown that the oxygen concentrations required to inhibit cytotoxicity of PR-104A in SiHa cultures are 10-fold lower than for tirapazamine.[2] This combination of effective inhibition of activation at normal tissue oxygen tensions with a bystander effect provides an attractive paradigm for exploiting tumor hypoxia. Clinical evaluation of PR-104, now in progress, will determine whether this promise translates into effective cancer therapy.

Acknowledgments

We thank Anke Tholl and Anderson Wang for developing the method for measuring PR-104H in cells; Sally Bai, Dan Li, and Chenbo Wu for assistance with *in vivo* studies; Drs. Steve Gatley, Paul Gonzales, and Stacy Hahn (TGen Drug Development Services, Scottsdale, AZ) for undertaking the Panc-01 tumor studies; Dr. Maryta Boyd for nuclear magnetic resonance spectroscopy; and Dr. Alice Richards (Gribbles Veterinary Pathology, Auckland, New Zealand) for evaluation of histopathology.

References

1. Brizel DM, Scully SP, Harrelson JM, et al. Tumor oxygenation predicts for the likelihood of distant metastases in human soft tissue sarcoma. Cancer Res 1996;56:941–3.
2. Vaupel P. Tumor microenvironmental physiology and its implications for radiation oncology. Semin Radiat Oncol 2004;14:198–206.
3. Subarsky P, Hill RP. The hypoxic tumour microenvironment and metastatic progression. Clin Exp Metastasis 2003;20:237–50.
4. Nordsmark M, Overgaard M, Overgaard J. Pretreatment oxygenation predicts radiation response in advanced squamous cell carcinoma of the head and neck. Radiother Oncol 1996;41:31–9.
5. Movsas B, Chapman JD, Hanlon AL, et al. Hypoxic prostate/muscle pO_2 ratio predicts for biochemical failure in patients with prostate cancer: preliminary findings. Urology 2002;60:634–9.
6. Koukourakis MI, Bentzen SM, Giatromanolaki A, et al. Endogenous markers of two separate hypoxia response pathways (hypoxia inducible factor 2α and carbonic anhydrase 9) are associated with radiotherapy failure in head and neck cancer patients recruited in the CHART randomized trial. J Clin Oncol 2006;24:727–35.
7. Brown JM, Wilson WR. Exploiting tumor hypoxia in cancer treatment. Nat Rev Cancer 2004;4:437–47.
8. Minchinton AI, Tannock IF. Drug penetration in solid tumours. Nat Rev Cancer 2006;6:583–92.
9. Hicks KO, Pruijn FB, Secomb TW, et al. Use of three-dimensional tissue cultures to model extravascular transport and predict *in vivo* activity of hypoxia-targeted anticancer drugs. J Natl Cancer Inst 2006;98:1118–28.
10. Brown JM, Giaccia AJ. The unique physiology of solid tumors: opportunities (and problems) for cancer therapy. Cancer Res 1998;58:1408–16.
11. Vaupel P, Kallinowski F, Okunieff P. Blood flow, oxygen and nutrient supply, and metabolic microenvironment of human tumors: a review. Cancer Res 1989;49:6449–65.
12. Halfpenny J, Wilson LD, Sun YH, et al. Concurrent chemo-radiotherapy with mitomycin C compared with perfluorocarbon in squamous cell cancer of the head and neck: final results of a randomized clinical trial. Int J Radiat Oncol Biol Phys 2005;61:119–28.
13. Cole S, Stratford IJ, Fielden EM, et al. Dual function nitroimidazoles less toxic than RSU 1069: selection of candidate drugs for clinical trial (RB 6145 and/or RB 190908). Int J Radiat Oncol Biol Phys 1992;22:545–8.
14. Brocker MA, Fischer GD, Graziano MJ, Gough AW. Retinal degeneration in rats induced by CI-1010, a 2-nitroimidazole radiosensitizer. Toxicol Pathol 1998;26:234–8.
15. Lee AE, Wilson WR. Hypoxia-dependent retinal toxicity of bioreductive anticancer prodrugs in mice. Toxicol Appl Pharmacol 2000;163:50–8.
16. Rischin D, Peters L, Fisher R, et al. Tirapazamine, cisplatin, and radiation versus fluorouracil, cisplatin, and radiation in patients with locally advanced head and neck cancer: a randomized phase II trial of the trans-tasman radiation oncology group (TROG 98.02). J Clin Oncol 2005;23:79–87.

17. Patterson LH, McKeown SR. AQ4N: a new approach to hypoxia-activated cancer chemotherapy. Br J Cancer 2000;83:1589–93.
18. Helsby NA, Wheeler SJ, Pruijn FB, et al. Effect of nitroreduction on the alkylating reactivity and cytotoxicity of the 2,4-dinitrobenzamide-5-aziridine CB 1954 and the corresponding nitrogen mustard SN 23862: distinct mechanisms of bioreductive activation. Chem Res Toxicol 2003;16:469–78.
19. Palmer BD, Wilson WR, Anderson RF, Boyd M, Denny WA. Hypoxia-selective antitumor agents. 14. Synthesis and hypoxic cell cytotoxicity of regioisomers of the hypoxia-selective cytotoxin 5-[*N,N*-bis(2-chloroethyl)amino]-2,4-dinitrobenzamide. J Med Chem 1996;39:2518–28.
20. Silva BG, Denny WA, Wilson WR. Nitro reduction as an electronic switch for bioreductive drug activation. Oncol Res 1997;9:357–68.
21. Wilson WR, Hicks KO, Pullen SM, et al. Bystander effects of bioreductive drugs: potential for exploiting pathological tumor hypoxia with dinitrobenzamide mustards. Radiat Res 2007;167:626–36.
22. Wilson WR, Pullen SM, Hogg A, et al. Quantitation of bystander effects in nitroreductase suicide gene therapy using three-dimensional cell cultures. Cancer Res 2002;62:1425–32.
23. Helsby NA, Ferry DM, Patterson AV, Pullen SM, Wilson WR. 2-Amino metabolites are key mediators of CB 1954 and SN 23862 bystander effects in nitroreductase GDEPT. Br J Cancer 2004;90:1084–93.
24. Denny WA, Atwell GJ, Yang S, et al., inventors; Auckland Uniservices Ltd., assignee. Novel nitrophenyl mustard and nitrophenylaziridine alcohols and their corresponding phosphates and their use as targeted cytotoxic agents. PCT WO 2005042471 A1. 2005.
25. Hay MP, Gamage SA, Kovacs MS, et al. Structure-activity relationships of 1,2,4-benzotriazine 1,4-dioxides as hypoxia-selective analogues of tirapazamine. J Med Chem 2003;46:169–82.
26. Atwell GJ, Denny WA. Synthesis of 3H- and 2H4-labelled versions of the hypoxia-activated pre-prodrug 2-[(2-bromoethyl)-2,4-dinitro-6-[2-(phosphonooxy)ethyl]amino]carbonyl]amino]ethyl methanesulfonate (PR-104). J Labelled Compounds Radiopharmaceuticals 2006;50:7–12.
27. Hicks KO, Pruijn FB, Sturman JR, Denny WA, Wilson WR. Multicellular resistance to tirapazamine is due to restricted extravascular transport: a pharmacokinetic/pharmacodynamic study in HT29 multicellular layer cultures. Cancer Res 2003;63:5970–7.
28. Tercel M, Lee AE, Hogg A, et al. Hypoxia-selective antitumor agents. 16. Nitroarylmethyl quaternary salts as bioreductive prodrugs of the alkylating agent mechlorethamine. J Med Chem 2001;44:3511–22.
29. MacPhail SH, Banath JP, Yu Y, Chu E, Olive PL. Cell cycle-dependent expression of phosphorylated histone H2AX: reduced expression in unirradiated but not X-irradiated G_1-phase cells. Radiat Res 2003;159:759–67.
30. Palmer BD, van Zijl P, Denny WA, Wilson WR. Reductive chemistry of the novel hypoxia-selective cytotoxin 5-[*N,N*-bis(2-chloroethyl)amino]-2,4-dinitrobenzamide. J Med Chem 1995;38:1228–41.
31. Thompson LH, Busch DB, Brookman K, Mooney CL, Glaser DA. Genetic diversity of UV-sensitive DNA repair mutants of Chinese hamster ovary cells. Proc Natl Acad Sci U S A 1981;78:3734–7.
32. Brookman KW, Lamerdin JE, Thelen MP, et al. ERCC4 (XPF) encodes a human nucleotide excision repair protein with eukaryotic recombination homologs. Mol Cell Biol 1996;16:6553–62.
33. Olive PL, Banath JP, Durand RE. The range of oxygenation in SiHa tumor xenografts. Radiat Res 2002;158:159–66.
34. Bernhardt KL, Durand RE. Quantifying transient hypoxia in human tumor xenografts by flow cytometry. Cancer Res 2004;64:6183–9.
35. Hulkham LA, Kyle AH, Baker JHE, Nykilchuk LK, Minchinton AI. Microregional effects of gemcitabine in HCT-116 xenografts. Cancer Res 2004;64:6537–41.
36. Tannock IF, Lee CM, Tunggal JK, Cowen DS, Egorin MJ. Limited penetration of anticancer drugs through tumor tissue: a potential cause of resistance of solid tumors to chemotherapy. Clin Cancer Res 2002;8:878–84.
37. Jang SH, Wientjes MG, Au JL. Determinants of paclitaxel uptake, accumulation and retention in solid tumors. Invest New Drugs 2001;19:113–23.
38. Denny WA, Wilson WR. Considerations for the design of nitrophenyl mustards as agents with selective toxicity for hypoxic tumor cells. J Med Chem 1986;29:879–87.
39. Monks NR, Biskey DC, East SJ, et al. DNA interstrand cross-linking and TP53 status as determinants of tumour cell sensitivity *in vitro* to the antibody-directed enzyme prodrug therapy ZD2767. Eur J Cancer 2002;38:1643–52.
40. Banath JP, Olive PL. Expression of phosphorylated histone H2AX as a surrogate of cell killing by drugs that create DNA double-strand breaks. Cancer Res 2003;63:4347–50.
41. Song BL, Wang D, Du Y, et al. The *in vivo* selection of the R-enantiomer of KS119W (VNP40541) as a potential anticancer agent. Proc Am Assoc Cancer Res 2006;47:1108.
42. Seow HA, Penketh PG, Shyam K, Rockwell S, Sartorelli AC. 1,2-Bis(methylsulfonyl)-1-(2-chloroethyl)-2-[1-(4-nitrophenyl)ethoxy]carbonyl]hydrazine: an anticancer agent targeting hypoxic cells. Proc Natl Acad Sci U S A 2005;102:9282–7.
43. Teicher BA, Chan V, Shih C, et al. Treatment regimens including the multitargeted antifolate LY231514 in human tumor xenografts. Clin Cancer Res 2000;6:1018–29.
44. Hardman WE, Moyer MP, Cameron IL. Efficacy of treatment of colon, lung and breast human carcinoma xenografts with: doxorubicin, cisplatin, irinotecan or topotecan. Anticancer Res 1999;19:2269–74.
45. Kovacs MS, Hocking DJ, Evans JW, et al. Cisplatin anti-tumour potentiation by tirapazamine results from a hypoxia-dependent cellular sensitization to cisplatin. Br J Cancer 1999;80:1246–51.
46. Papadopoulou MV, Bloomer WD. NLCQ-1 (NSC 708257): exploiting hypoxia with a weak DNA-intercalating bioreductive drug. Clin Cancer Res 2003;9:6714–20.
47. Koong AC, Mehta VK, Le QT, et al. Pancreatic tumors show high levels of hypoxia: regarding Koong, et al. IJROBP 2000;48:919–22. Int J Radiat Oncol Biol Phys 2000;48:919–22.
48. Vaupel P, Thews O, Kelleher DK. Pancreatic tumors show high levels of hypoxia: regarding Koong, et al. IJROBP 2000;48:919–2. Int J Radiat Oncol Biol Phys 2001;50:1089–100.
49. Parker C, Milosevic M, Toi A, et al. Polarographic electrode study of tumor oxygenation in clinically localized prostate cancer. Int J Radiat Oncol Biol Phys 2004;58:750–7.
50. Carnell DM, Smith RE, Daley FM, et al. An immunohistochemical assessment of hypoxia in prostate carcinoma using pimonidazole: implications for radioresistance. Int J Radiat Oncol Biol Phys 2006;65:91–9.